



HAL
open science

Impact of dose-rate on the low-dose hyper-radiosensitivity and induced radioresistance (HRS/IRR) response.

Charles Thomas, Martin Jennifer, Clément Devic, Elke Bräuer-Krisch, Michel Diserbo, Juliette Thariat, Nicolas Foray

► To cite this version:

Charles Thomas, Martin Jennifer, Clément Devic, Elke Bräuer-Krisch, Michel Diserbo, et al.. Impact of dose-rate on the low-dose hyper-radiosensitivity and induced radioresistance (HRS/IRR) response.. International Journal of Radiation Biology, 2013, 89 (10), pp.813-22. 10.3109/09553002.2013.800248 . inserm-00868975

HAL Id: inserm-00868975

<https://inserm.hal.science/inserm-00868975v1>

Submitted on 13 Jun 2014

HAL is a multi-disciplinary open access archive for the deposit and dissemination of scientific research documents, whether they are published or not. The documents may come from teaching and research institutions in France or abroad, or from public or private research centers.

L'archive ouverte pluridisciplinaire **HAL**, est destinée au dépôt et à la diffusion de documents scientifiques de niveau recherche, publiés ou non, émanant des établissements d'enseignement et de recherche français ou étrangers, des laboratoires publics ou privés.

Impact of dose-rate on the low-dose hyper-radiosensitivity and induced radioresistance (HRS/IRR) response#

Charles Thomas^{1*}, Jennifer Martin¹, Clément Devic¹, Elke Bräuer-Krisch², Michel Diserbo³, Juliette Thariat⁴, Nicolas Foray¹

¹Institut National de la Santé et de la Recherche Médicale (INSERM) U1052, groupe de radiobiologie, Lyon, France.

²European Synchrotron Radiation Facility, Grenoble, France.

³Institut de Recherche Biomédicale des Armées (IRBA), BP 87, 38702 La Tronche, France.

⁴Centre Antoine Lacassagne, Radiotherapy unit, Nice, France.

#The authors dedicate this work to Bernard Fertil for his contribution to radiobiology.

Figures: 4

Tables: 4

Running title: The HRS/IRR response does not depend on dose-rate

Keywords: Hyper-radiosensitivity (HRS) response, induced radioresistance (IRR) response, dose-rate, DSB repair, tumour cells, radiotherapy.

*Correspondence: Charles Thomas, Inserm U1052, Centre de Recherche en Cancérologie de Lyon, 28 Rue Laënnec, 69008 Lyon, France. Email: charles.thomas1@sfr.fr, tel: (33) 6 98 26 16 03

Abstract

Purpose: To ask whether dose-rate influences low-dose hyper-radiosensitivity and induced radioresistance (HRS/IRR) response in rat colon carcinoma PRO and REG cells.

Methods: Clonogenic survival was applied to tumourigenic PRO and non-tumourigenic REG cells irradiated with ^{60}Co γ -rays at 0.0025–500 mGy.min⁻¹. Both clonogenic survival and non-homologous end-joining (NHEJ) pathway involved in DNA double-strand breaks (DSB) repair assays were applied to PRO cells irradiated at 25 mGy.min⁻¹ with 75 kV X-rays only.

Results: Irrespective of dose-rates, marked HRS/IRR responses were observed in PRO but not in REG cells. For PRO cells, the doses at which HRS and IRR responses are maximal were dependent on dose-rate; conversely exposure times during which HRS and IRR responses are maximal (t_{HRSmax} and t_{IRRmax}) were independent of dose-rate. The t_{HRSmax} and t_{IRRmax} values were $23\pm 5\text{s}$ and $66\pm 7\text{s}$ [mean \pm standard error of the mean (SEM), n=7], in agreement with literature data. Repair data show that t_{HRSmax} may correspond to exposure time during which NHEJ is deficient while t_{IRRmax} may correspond to exposure time during which NHEJ is complete.

Conclusion: HRS response may be maximal if exposure times are shorter than t_{HRSmax} irrespective of dose, dose-rate and cellular model. Potential application of HRS response in radiotherapy is discussed.

Introduction

It is now well documented that cells irradiated at single low-dose fraction can show marked hyper-radiosensitivity (HRS) and induced radioresistance (IRR) response (Table I). The HRS/IRR response is a representative example of a non-linear dose-dependent event. The HRS/IRR response was originally observed *in vivo* in mice using acute skin tissue damage as an endpoint (Joiner et al. 1986). Thereafter, the HRS response, mostly observed by using *in vitro* survival assay in single tumour cells, was shown to result in a significant reduction of about 25 % cell survival between 0.1 and 0.8 Gy. The dose at which the maximal HRS response is observed (D_{HRSmax}) depends on the cell line (Table I). The HRS response generally occurs in tumour or transformed cells (Marples and Collis 2008). At doses higher than D_{HRSmax} , cell survival increases progressively and this phenomenon was called IRR response. Despite a number of studies, the mechanisms of the HRS and IRR responses, whether taken separately or together, remain unclear. It has been suggested that the HRS response may depend upon changes in chromatin conformation (Joiner et al. 2001), failure of the Ataxia Telangiectasia mutated protein (ATM)-dependent G_2/M checkpoint (Marples et al. 2004), or defects in DNA double-strand breaks (DSB) (Vaganay-Juery et al. 2000, Short et al. 2005). It was notably suggested that the HRS response may reflect apoptotic death of tumour cells that failed to arrest in cell cycle whereas the IRR response may reflect early cell cycle G_2 -phase arrest allowing time for repair and increased cell survival (Marples and Collis 2008). In 2008, we pointed out that the HRS response may be caused by impairments in the non-homologous end-joining (NHEJ) repair pathway that targets G_1 cells and in lack of control of the RAD51-dependent recombination repair pathway that targets S- G_2/M cells; the consequences of such impairments are failure to arrest in the cell cycle, propagation of damage through the cell cycle, mitotic death, but not p53-dependent apoptosis (Thomas et al. 2008).

The HRS/IRR response is more marked in cells displaying genomic instability: in fact, this response was mostly observed in tumour and in some transformed normal cell lines (Table I). Furthermore, we have previously reported that human and rodent tumourigenic cells with high metastatic potential preferentially show the HRS response (Thomas et al. 1997, 2008). We have therefore suggested that the HRS response may find applications in radiotherapy, notably for unvascularised and isolated

micrometastasis (Thomas et al. 2001, 2007). On the other hand, the occurrence of the HRS/IRR response in primary normal cells is still controversial and may depend on the differentiation and/or proliferation status. As an example, six among nine primary explants of uroepithelium showed HRS/IRR response with a 14 days post-irradiation proliferative assay as endpoint (Mothersill et al. 1995). The HRS/IRR response assessed by micronuclei assay was also observed in about 10% of primary keratinocytes and fibroblasts from cervix carcinoma patients (Slonina et al. 2007).

Interestingly, the literature shows that the HRS/IRR response of tumour cells irradiated with low-energy transfer (LET) radiation was investigated at dose-rates ranging from 0.18 to 2.43 Gy.min⁻¹ (Table I). These data raise the question of a dose-rate dependence of the HRS/IRR response. In order to answer this question, we investigated clonogenic cell survival at seven dose-rates (from 0.0025 to 500 mGy.min⁻¹) in two rat colon carcinoma cell sublines (PRO/REG) that were shown to be HRS positive and negative, respectively (Thomas et al. 2008).

Materials and methods

Cells and irradiation

Rat colon carcinoma PRO and REG cells were kindly provided by Dr F. Martin (Dijon, France). PRO and REG sublines were isolated from the parental tumour cell line DHD-K12, established from dimethylhydrazine-induced colon carcinoma in syngeneic BDIX rats (Martin et al. 1983). PRO and REG sublines were isolated according to their sensitivity to trypsin-mediated detachment from plastic surface (PRO subline is more trypsin-resistant than REG subline). When grafted subcutaneously in BDIX rats, REG cells produced regressive tumours disappearing within 3-4 weeks while PRO cells produced progressive tumours in 60 % of animals with metastases to lungs, kidney or lymph nodes (Martin et al. 1983). PRO and REG sublines were cultured in Roswell Park Memorial Institute (RPMI) 1640 medium with 2 mM glutamine, 10 % decomplexed fetal bovine serum, 1 % [4-(2-hydroxyethyl)-1-piperazineethanesulfonic acid] (HEPES) and antibiotics (1 % penicillin, streptomycin) (Gibco-Invitrogen-France, Cergy-Pontoise, France). Cells were mycoplasma-free and maintained at 37°C at 5 % CO₂ for no more than five passages after defrost. For all the assays described below, confluent PRO and REG cultures were softly detached with 0.025 % trypsin and 0.02 % ethylenediaminetetraacetic acid (EDTA) (Gibco-Invitrogen-France, Cergy-Pontoise, France) to obtain single cell suspensions. Since the HRS/IRR response is suppressed under condition of increased cell-cell contact (Chandna et al. 2002), the number of aggregates (no more than 5 cells) was kept as low as possible. Irradiations were performed at European Synchrotron Radiation Facility (ESRF, Grenoble, France) with X-rays produced by a clinical irradiator (75 kV, 14 mA) at a dose rate of 25 mGy/min and at Institut de Recherche Biomédicale des Armées (IRBA, Grenoble, France) with ⁶⁰Co γ -rays at dose-rates of 230, 60, 44, 25, 0.3 or 0.0025 mGy.min⁻¹. This range of dose-rate corresponds to space radiation (0.0025 mGy.min⁻¹), nuclear medicine (0.3 mGy.min⁻¹), radiodiagnosis (25, 44, 60 mGy.min⁻¹) and radiotherapy (230 mGy.min⁻¹). These four groups of dose-rate are evenly distributed on log scale. The 25 mGy.min⁻¹ dose-rate was chosen to evaluate cell survival at two different clinically relevant radiation type (Cobalt 60 γ -rays and 75 kV X-rays). Dose and their homogeneity in the irradiation field were routinely verified with Physikalisch Technische Werkstätten (PTW) ionization chambers

(0.3 cm³ type TM23332 for dose-rates higher than 25 mGy.min⁻¹ and 30 cm³ type TM23361 for dose-rates lower than 25 mGy.min⁻¹ at IRBA and semiflex chamber type TW31010–03907 for dose-rate of 25 mGy.min⁻¹ at ESRF). The relative dose error was 10 %. The error committed on exposure times (given digitally) was negligible. For all the dose-rates applied in this study, the exposure times were always shorter than 10 min (Table II).

Clonogenic survival assay

Clonogenic survival was assessed as previously described (Thomas et al. 2008). Briefly, 250 cells were seeded in six well plates and irradiated 24 h after plating at various dose-rates. Colonies were fixed and stained with standard crystal violet solution (Sigma-Aldrich-France, l'Isle d'Abeau, France) after ten days incubation without change of medium. Only colonies showing more than 50 cells were considered. Plating efficiencies of unirradiated REG and PRO cells at IRBA were 39 ± 6 % [mean \pm standard error of the mean (SEM), n = 8 independent experiments] and 25 ± 2 % (mean \pm SEM, n = 17 independent experiments), respectively. Plating efficiencies of unirradiated REG and PRO cells at ESRF were 29 ± 3 % (mean \pm SEM, n = 3 independent experiments) and 14 ± 1 % (mean \pm SEM, n = 2 independent experiments), respectively. The impact of cell proliferation before irradiation on HRS response was previously investigated; we showed that the HRS response was similar in PRO cells whether irradiated 2 h or 24 h after plating; cell multiplicity (i.e. the number of cells per colony-forming unit) 24 h after plating was found to be close to one (Thomas et al. 2008).

Survival curves analysis

Using the JMP software (version 2.0.5. SAS institute, Cary, NC, USA), the surviving fractions (SF) were fitted to two models: the one population linear-quadratic (LQ) model and the induced repair (IR) model (Thomas et al. 2008) defined by, respectively:

$$(1) \text{ SF}(D) = e^{-(\alpha \cdot D + \beta \cdot D^2)}$$

$$(2) \text{ SF (D)} = e^{-\alpha_r \left[1 + \left(\frac{\alpha_s}{\alpha_r} - 1 \right) \cdot e^{-\frac{D}{d_c}} \right] \cdot D - \beta_r \cdot D^2}$$

The IR model is a modified version of the LQ model in which the α term is dependent on dose (D): at very low doses, α is large, and it decreases with increasing dose in an exponential manner at a rate determined by a constant d_c . The parameter α_s represents the initial slope of the survival curve at very low doses; α_r represents the initial slope of the survival curve extrapolated from the conventional high-dose response described by the LQ model; d_c represents the dose that induced the change from HRS to IRR response and β_r represents the distal slope of the survival curve. The occurrence of the HRS/IRR response is mathematically deduced from α_s and α_r values that do not coincide and d_c values significantly greater than zero (Table II). Since some data reported in Table I were not always fitted to the IR model, we deliberately chose to rename the d_c parameter D_{HRSmax} since it corresponds to the maximal extent of the HRS response. Similarly, we defined the D_{IRRmax} parameter that corresponds to the maximal extent of the IRR response (Table I).

Immunofluorescence assay

The assay which is described elsewhere (Thomas et al. 2008), was applied with minor modifications to measure the number of γ -pH2AX foci per cell 15 min, 1 h, 4 h and 24 h after irradiation. Briefly, 10^4 cells were seeded on slides in six well plates and incubated for 24 h in complete medium at 37° C. After irradiation at 75 kV X-rays at 10 mGy (24 s) and 100 mGy (240 s), plates were incubated at 37° C for 10 min and 24 h. Cells were then fixed in paraformaldehyde solution for 15 min at room temperature and permeabilized for 90 s at 4° C in lysis solution [20 mM HEPES) (pH 7.4), 50 mM NaCl, 3 mM MgCl₂, 300 mM sucrose, 0.5 % Triton X-100] (Sigma-Aldrich-France, l'Isle d'Abeau, France). Primary antibody incubations were performed for 40 min at 37°C. Anti- γ -pH2AX^{ser139} antibody (#05636; Upstate Biotechnology-Euromedex, Mundolsheim, France) was used at 1:800. Incubation with anti-mouse fluorescein (green) secondary antibody was performed at 1:100 at 37°C for 20 min. Slides were mounted in 4',6-diamidino-2-phenylindole (DAPI)-stained Vectashield (Abcys, Paris, France) and the number of γ -pH2AX foci per cell in 126-

209 cells (15 min experiments) or 142-198 cells (24 h experiments) were examined with Olympus BX51 fluorescence microscope. DAPI staining permitted to indirectly evaluate yield of G₁ cells (nuclei with homogeneous DAPI staining), S cells (nuclei showing numerous γ -pH2AX foci), G₂ cells (nuclei with heterogeneous DAPI staining) and metaphase (visible chromosomes). DAPI staining permitted also to quantify the percentage of cells with micronuclei by examining 100 cells at least. In order to avoid any bias by using imaging analysis software, the number of foci per cell was determined after eye-scoring in about 50 cells in G₀/G₁ per slide.

Results

HRS/IRR response of PRO cells irradiated with ^{60}Co γ -rays. In 2008, we demonstrated the existence of a HRS/IRR response in PRO cells but not in REG cells irradiated at $500 \text{ mGy}\cdot\text{min}^{-1}$. The D_{HRSmax} value that reflects the transition between the HRS and IRR response (i.e. the lowest survival data) was $190 (\pm 8) \text{ mGy}$ (Thomas et al. 2008). This dose corresponds to an exposure time of $23 (\pm 1) \text{ s}$ at $500 \text{ mGy}\cdot\text{min}^{-1}$ (Table I). In order to examine whether dose-rate influences the HRS/IRR response, we investigated clonogenic survival of PRO cells irradiated at six different dose-rates between 0.0025 and $230 \text{ mGy}\cdot\text{min}^{-1}$. For all the dose-rates applied in this study, a HRS/IRR response was systematically observed in PRO cells (Fig. 1A-F). Since the distal part of the survival curves obtained at 0.3 and $0.0025 \text{ mGy}\cdot\text{min}^{-1}$ showed negative βr parameter with the IR model (Table III), all data were fitted to a smooth function (Fig. 1A-F). Irrespective of the dose-rates, the HRS/IRR response was observed systematically, but not at the same dose range. For example, the lowest survival was $86 \pm 1 \%$ irrespective of dose-rate, but D_{HRSmax} ranged between 190 mGy at $500 \text{ mGy}\cdot\text{min}^{-1}$ and 0.00071 mGy at $0.0025 \text{ mGy}\cdot\text{min}^{-1}$ (Table IV). The D_{HRSmax} values appeared to be a linear function of dose-rate with $D_{\text{HRSmax}} = 0.4428 \times \text{dose-rate}$ ($R^2 = 0.89$) (Fig. 2A). The slope of this linear function corresponds to the exposure time required for the maximal HRS response. For convenience, we called it t_{HRSmax} . Its average value was $0.4428 \pm 0.05 \text{ min}$ or $26.57 \pm 3 \text{ s}$, and independent of dose-rate (Fig. 2B). Similarly, if D_{IRRmax} and t_{IRRmax} are defined as the dose and the exposure time required for the maximal IRR response, respectively, our data showed that D_{IRRmax} is linearly dependent on dose-rate with $D_{\text{IRRmax}} = 0.997 \times \text{dose-rate}$ ($R^2 = 0.99$) (Fig. 2C). The slope t_{IRRmax} was found to be $0.997 \pm 0.07 \text{ min}$ or $59.8 \pm 4.2 \text{ s}$, and independent of dose-rate (Fig. 2D). Thus, it appears that the maximal HRS and IRR responses in PRO cells correspond to exposure times that are independent of dose-rates.

In agreement with our previous data obtained at $500 \text{ mGy}\cdot\text{min}^{-1}$, it is noteworthy that REG cells did not show marked HRS/IRR response at $44 \text{ mGy}\cdot\text{min}^{-1}$ and $0.0025 \text{ mGy}\cdot\text{min}^{-1}$ (Fig. 1C and 1F, respectively). Conversely, REG cells displayed significant radio-stimulation at $0.0025 \text{ mGy}\cdot\text{min}^{-1}$ (Fig. 1F). Such very low dose-rate is known to stimulate the division potential in normal cells (e. g. Croute et al. 1986, Planel et al. 1987). However, these hormetic-like responses and their possible

cellular mechanisms – that were recently reviewed (Szumiel 2012) – are beyond the scope of this paper.

Comparison with the literature. We reviewed the HRS/IRR responses obtained in the literature from 1993 to 2012 (Table I). As a first step, only low-LET radiation (X- and γ -rays) data obtained at single dose-rate with short exposure times less than 10 min were considered. With regard to the HRS/IRR response parameters, no significant difference was observed between human and rodent cells. By pooling rodent and human data shown in Table I, the HRS/IRR responses were obtained at an average dose-rate of $1000 \text{ mGy}\cdot\text{min}^{-1}$. At such dose-rate, the D_{HRSmax} and D_{IRRmax} values obtained in the literature are in agreement with our data (Fig. 1A and C). The t_{HRSmax} value obtained in the literature [$23 \pm 4 \text{ s}$ (mean \pm SEM, $n = 25$)] was not significantly different from the experimental t_{HRSmax} value obtained in this study [$23.4 \pm 5.3 \text{ s}$ (mean \pm SEM, $n = 7$)] (Table IV). Similarly, the t_{IRRmax} value obtained in the literature [$59 \pm 12 \text{ s}$ (mean \pm SEM, $n = 25$)] was not significantly different from the experimental t_{IRRmax} value obtained in this study [$66 \pm 7.1 \text{ s}$ (mean \pm SEM, $n = 7$)] (Table IV). By pooling literature and our data, over a very large range of dose-rates ($0.0025 - 2430 \text{ mGy}\cdot\text{min}^{-1}$) t_{HRSmax} and t_{IRRmax} were found to be $23 \pm 3 \text{ s}$ and $60 \pm 9 \text{ s}$ [mean \pm SEM ($n = 32$)], respectively.

HRS/IRR response of PRO cells irradiated with 75 kV X-rays. Since radiodiagnosis exams like computed tomography (CT) scans involve low-energy X-rays rather than high-energy γ -rays, we examined whether the HRS/IRR response of PRO cells also exists with 75 kV X-rays. With regard to dose-rate, we chose to work at $25 \text{ mGy}\cdot\text{min}^{-1}$ since this dose-rate generally applied in CT scan exams. Figure 3A shows that in the 5-100 mGy range, the HRS/IRR response occurs in PRO cells. Although the extent of the HRS response in PRO cells appeared to be larger with 75 kV X-rays than with ^{60}Co γ -rays, the survival data were not found significantly different (Figure 3A). Accordingly, the HRS and the IRR response parameters fitted with the IR model were found similar with 75 kV X-rays and ^{60}Co γ -rays (Table III). Finally we confirmed that REG cells irradiated with 75 kV X-rays did not display significant HRS/IRR response (data not shown).

DSB repair features of HRS/IRR response. Thereafter, by using 75 kV X-rays delivered at 25 mGy.min⁻¹, we examined the radiation-induced DSB reflected by γ -H2AX foci in two representative conditions: after 10 mGy, corresponding to the maximal HRS response (D_{HRSmax}) and an exposure time lower than t_{HRSmax} ; after 100 mGy, corresponding to dose higher than the maximal IRR response (doses higher than D_{IRRmax}) and exposure time longer than t_{IRRmax} . Figure 3B showed that for both doses, the kinetics of appearance/disappearance of γ -H2AX foci elicited the same biphasic shape: 1) an increase of the number of γ -H2AX foci corresponding to the recognition of radiation-induced DSB managed by NHEJ; 2) a decrease of the number of γ -H2AX foci corresponding to the repair of recognized DSB. However, while the maximal number of γ -H2AX foci ranged from 7 to 11 nuclear foci for both doses, the incubation times at which it was reached differed significantly, i.e. 4 h and 1 h post-irradiation after a dose of 10 mGy and 100 mGy, respectively. Furthermore, while the DSB repair is completed after 100 mGy, the DSB induced by 10 mGy appeared to be more severe with 5.5 ± 0.7 residual γ -H2AX foci 24 h after irradiation (Figure 3B). These data suggest that t_{HRSmax} may be associated with deficient NHEJ repair and maximal HRS response while t_{IRRmax} may be associated with full NHEJ repair and maximal IRR response.

Discussion

Impact of dose-rate on the HRS/IRR response

By investigating one of the largest ranges of dose-rates applied in HRS/IRR studies, our data show that the maximal HRS and IRR responses obtained with low-LET radiation correspond to exposure times of about 20 s and 60 s, respectively. To our knowledge, the impact of dose-rate and exposure time on the HRS/IRR response have not been investigated *per se*, notably with short exposure times less than 10 min. Exposure time is basically dependent on dose and dose-rate since these three parameters are linked mathematically. The dose-rates applied in the published studies ranging from 0.18 to 2.43 Gy.min⁻¹ (Table I), have rarely been explained: their choice generally results from a practical compromise between the availabilities of the irradiator in the laboratory, a short exposure time to avoid artifacts and the possibility to expose cells during a minimal time. For example, some authors used several dose-rates for completing a single survival curve (e.g. Marples and Joiner 1993; Martin et al. 2009). We deliberately chose not to include the studies using several dose-rates in our review shown in Table I. Similarly, HRS/IRR responses obtained with long exposure times (generally longer than one hour) were not considered (e.g. Enns et al. 2004).

Some HRS/IRR responses were also observed with other radiation than X- or γ -rays. This is notably the case of neutrons (Dionnet et al. 2000), α -rays (Tsoulou et al. 2001), protons (Petrovic et al. 2010), heavy ions (Xue et al. 2009) and β -rays (Wéra et al. 2012). Interestingly, D_{HRSmax} , D_{IRRmax} , t_{HRSmax} , t_{IRRmax} are also in agreement with the values range of our review (Table I), which consolidates our conclusions showing that the maximal HRS and IRR responses would correspond, (by pooling literature and our data), to average exposure times of 31 ± 8 s (SEM, n = 35) and 58 ± 9 s (SEM, n = 35) respectively, irrespective of the radiation type (low and high-LET radiation). Thus our data suggest that the HRS response is not limited to low-doses since t_{HRSmax} can theoretically be reached with high-doses. Accordingly, tumour cells irradiated at 2 Gy with protons at 15 Gy.min⁻¹ (exposure time = 8 s) showed HRS response (Petrovic et al. 2012). However, since most HRS/IRR responses were obtained with low-LET radiation corresponding to cell survival of

75 ± 18 % (mean ± SD, n = 28) with doses ranging from 100 to 800 mGy (Table I), we stressed that the validity of the HRS/IRR response may not be relevant for higher doses and lower cell survival.

Biological significance of t_{HRSmax}

The findings that t_{HRSmax} and t_{IRRmax} are constant and common to human and rodent cells, tumour and transformed normal cells suggest that exposure times corresponding to the maximal HRS and IRR responses may not entirely depend on cellular parameters like cellular model or cell death pathways. Furthermore, a drastic decrease of cell survival was shown to be correlated with DSB repair impairments with a number of cellular models and conditions (e.g. Joubert et al. 2008). In mammalian cells, DSB are mainly recognized and repaired by the NHEJ pathway. Particularly, alterations in NHEJ induce hyper-radiosensitivity at high-doses. This is the case of ATM-, ligase (LIG) 4-, DNA-protein kinase (PK)-mutated cell lines that exhibit a survival fraction at 2 Gy (SF2) of about 1 % (Joubert et al. 2008). Interestingly, the α parameter of the LQ model and the surviving fractions corresponding to these hyper-radiosensitive cell lines are very similar to those observed in the initial part of the survival curve in PRO cells and in other HRS-positive cell lines sorted in Table I. We suggest therefore that the $[0 - t_{\text{HRSmax}}]$ exposure time interval may correspond to an incapacity of NHEJ to recognize and repair efficiently the induced DSB, as it is the case for the ATM-, LIG4-, DNA-PK-mutated cells. It was shown that the ATM kinase produces a cascade of phosphorylations of proteins involved in the radiation response (Foray et al. 2003). The NHEJ repair pathway requires several steps such as: (1) DSB recognition, (2) interaction between ATM and γ -H2AX, (3) complete H2AX phosphorylation. In our hands, at least 10 min post-irradiation are required to observe the maximal number of γ -H2AX foci. Besides, some authors applied 30 min post-irradiation to assess the number of recognized DSB (e.g. Joubert et al., 2008). Hence, DSB recognition and repair steps likely require much more than 20 s. Since residual DSB is observed 24 h after irradiation at 10 mGy delivered either at 25 mGy.min⁻¹ (exposure time of 24 s) (this study) or at 70 mGy.min⁻¹ (exposure time 8.5 s) (Grudzenski et al. 2010), we suggest that t_{HRSmax} may be consistent with the time corresponding to deficient NHEJ repair.

Biological significance of t_{IRRmax}

With regard to the second part of the survival curve ranging from t_{HRSmax} to t_{IRRmax} , an increase of cell survival is observed: induced-radioresistance (IRR) is the major interpretation of this part of the survival curve (Krueger et al. 2007b). The t_{IRRmax} exposure time would therefore correspond to the time necessary for a fully active NHEJ pathway. Our data in figure 3B show that NHEJ repair is complete 24 h after irradiation at 100 mGy delivered at 25 mGy.min⁻¹ which corresponds to an exposure time larger than t_{IRRmax} . Accordingly, t_{IRRmax} may be compatible with kinetic of change in chromatin structure and nucleo-shuttling of pATM forms (Bakkenist and Kastan 2003), the earliest time to detect γ -H2AX foci after irradiation (Rothkamm and Löbrich 2003) and the time required for induced repair after low-dose X-rays [e.g. 68 s or 80 mGy delivered at 70 mGy.min⁻¹ (Grudzenski et al. 2010)]. Altogether, our data are compatible with three exposure time phases and N-shaped dose-response curve regarding DSB and cell survival (Figure 4):

- $t < t_{HRSmax}$: incomplete DSB recognition by NHEJ and decrease of cell survival (HRS response)
- $t_{HRSmax} < t < t_{IRRmax}$: progressive activation of NHEJ and increase of cell survival (IRR response)
- $t > t_{IRRmax}$: all DSB are recognized but they are so numerous that they cannot be all repaired; decrease of cell survival (beyond the HRS/IRR response).

Potential impact of the HRS/IRR response in radiotherapy

Our findings suggest that significant decrease of cell survival could be reached independently of dose-rate provided that exposure times are shorter than 30 s. This may be notably the case of the cyberknifeTM radiotherapy technique that delivers non-uniform patterns of intermittent radiation using a compact miniaturized 6 MV nominal linear accelerator with high doses-rates of 4,6, or 8 Gy.min⁻¹. The dose per fraction is delivered using 80-150 non-coplanar sequential mini-beams with < 0.1% leakage at 1 m from the beam path. For example, for a dose per fraction of about 7 Gy to the brain, the peripheral dose is less than 5 mGy at 80 cm from the target (Di Betta et al. 2010).

Interestingly, cyberknife delivers a single fraction of the total dose in 1–36 s with an interval between two beams of 5 s (Murphy et al. 2007). Furthermore, Lin and Wu reported that not all 2 Gy fractions are equivalent: human and rodent cells irradiated with ^{60}Co γ -rays at 1.3–1.5 Gy.min⁻¹ in 10 fractions of 0.2 Gy (corresponding to about 8 s per fraction with an interval of 16 s between fractions) showed higher radiosensitivity than a single fraction of 2 Gy (corresponding to an exposure time of 86 s at 1.4 Gy.min⁻¹) (Lin and Wu 2005). Thus data suggest that intermittent irradiation delivered in multiple fractions or continuous irradiation delivered in a single fraction with exposure time per fraction shorter than 20 s may show maximal HRS response independently of dose-rate. However, further investigations are required to examine whether the time between fractions impacts significantly on the HRS response.

Finally and consistently with our previous reports (Thomas et al. 1997, 2001, 2007, 2008), we suggest that the HRS response may be relevant to target unvascularised micrometastases with peripheral doses received at a distance from the clinical target volume irradiated with intermittent radiation. In the context of oligometastatic disease, local ablative stereotactic irradiation can be used to eradicate gross tumour while the potential microscopic disease is managed using systemic treatments (chemotherapy) or left untreated (Thariat et al. 2012). We suggest that the HRS response driven by short exposure times such as used with stereotactic radiotherapy may find also application to manage micrometastatic disease at distance from the irradiated gross tumour. More experimental and clinical investigations with additional highly metastatic human cell lines will be needed to verify this medical hypothesis.

Acknowledgements

We are grateful to the reviewers for their helpful comments and to Dr. Christian Mazars and its team [Unité Mixte de Recherche (UMR) Université Paul Sabatier (UPS)-Centre National de la Recherche Scientifique (CNRS) 5546, Toulouse] for helpful discussions. We thank also madame Beaufrère for her assistance in editing English. This work is supported by the Alliance de la Vie et de la Santé (AVIESAN), the Agence Nationale de la Recherche (ANR), the Institut National du Cancer (INCa), the Centre National d'Etudes Spatiales (CNES) and the Association pour la Recherche sur l'ataxie Telangiectasie (APRAT).

Conflict of interest statement

The authors declare that there are no conflicts of interest.

References

Barkowiak D, Högner S, Nothdurft W, Röttinger EM. 2001. Cell cycle and growth response of CHO cells to X-irradiation: threshold-free repair at low-doses. *International Journal of Radiation Oncology Biology Physics* 50: 221-227.

Beauchesne P, Bertrand S, Branche R, Linke SP, Doré JF, Pedeux RM. 2003. Human malignant glioma cell lines are sensitive to low radiation doses. *International Journal of Cancer* 105: 33-40.

Bakkenist CJ, Kastan MB. 2003. DNA damage activates ATM through intermolecular autophosphorylation and dimer dissociation. *Nature* 421: 499-506.

Chandna S, Dwarakanath BS, Khaitan D, Mathew TL, Jain V. 2002. Low-dose radiation hypersensitivity in human tumour cell lines: effects of cell-cell contact and nutritional deprivation. *Radiation Research* 157:516-525.

Croute F, Vidal S, Soleilhavoud JP, Vincent C, Serre G, Planel H. 1986. Effects of a very low dose rate of chronic ionizing radiation on the division potential of human embryonic lung fibroblasts in vitro. *Experimental Gerontology* 21: 1-11.

Di Betta E, Fariselli L, Bergantin A, Locatelli F, Del Vecchio A, Broggi S, Fumagalli ML. 2010. Evaluation of the peripheral dose in stereotactic radiotherapy and radiosurgery treatments. *Medical Physics* 37, 3587-3594.

Dionnet C, Tchirkov A, Alard JP, Arnold J, Dhermain J, Rapp M, Bodez V, Tamain JC, Monbel I, Malet P, Kwiatkowski F, Donnarieix D, Veyre A, Verelle P. 2000. Effects of low-dose neutrons applied at reduced dose rate on human melanoma cells. *Radiation Research* 154: 406-411.

Edin NJ, Olsen DR, Stokke T, Pettersen EO. 2007. Recovery of low-dose hyper-radiosensitivity following a small priming dose depends on priming dose-rate. *International Journal of Low Radiation* 4: 69-86.

Enns L, Bogen KT, Wizniak J, Murtha AD, Weinfeld M. 2004. Low-dose radiation hypersensitivity is associated with p53-dependent apoptosis. *Molecular Cancer Research* 2: 557-566.

Foray N, Marot D, Gabriel A, Randrianarison V, Carr AM, Perricaudet M, Ashworth A, Jeggo P. 2003. A subset of ATM- and ATR-dependent phosphorylation events requires the BRCA1 protein. *EMBO Journal* 22: 2860-2871.

Grudzenski S, Raths A, Conrad S, Rube CUE, Löbrich M. 2010. Inducible response required for repair of low-dose radiation damage in human fibroblasts. *Proceedings of the National Academy of Sciences, USA* 107: 14205-14210.

Joiner MC, Denekamp J, Maughan RL. 1986. The use of 'top-up' experiments to investigate the effect of very small doses per fraction in mouse skin. *International Journal of Radiation Biology* 49: 565-580.

Joiner MC, Marples B, Lambin P, Short SC, Turesson I. 2001. Low-dose hypersensitivity: current status and possible mechanisms. *International Journal of Radiation Oncology Biology Physics* 49: 379-389.

Joubert A, Zimmerman KM, Bencokova, Z, Gastaldo J, Rénier W, Chavaudra N, Favaudon V, Arlett CF, Foray N. 2008. DNA double-strand break repair defect in syndromes associated with acute radiation response: involvement of DNA-PK-and MRE11-dependent pathways. *International Journal of Radiation Biology* 84: 107-125.

- Krueger SA, Joiner MC, Weinfeld M, Piasentin E, Marples B. 2007a. Role of apoptosis in low-dose hyper-radiosensitivity. *Radiation Research* 167: 260-267.
- Krueger SA, Collis SJ, Joiner MC, Wilson GD, Marples B. 2007b. Transition in survival from low-dose hyper-radiosensitivity to increased radioresistance is independent of activation of ATM SER1981 activity. *International Journal of Radiation Oncology Biology Physics* 69: 1262-1271.
- Lambin P, Marples B, Fertil B, Malaise EP, Joiner MC. 1993. Hypersensitivity of a human tumour cell line to very low radiation doses. *International Journal of Radiation Biology* 63: 639-650.
- Lambin P, Malaise EP, Joiner MC. 1996. Might intrinsic radioresistance of human tumour cells be induced by radiation ? *International Journal of Radiation Biology* 69: 279-290.
- Lin PS, Wu A. 2005. Not all 2 Gray radiation prescriptions are equivalent: cytotoxic effect depends on delivery sequences of partial fractionated doses. *International Journal of Radiation Oncology Biology Physics*. 63, 536–544.
- Marples B, Joiner MC. 1993. The response of Chinese Hamster V79 cells to low radiation doses: evidence of enhanced sensitivity of the whole cell population. *Radiation Research* 133: 41-51.
- Marples B, Wouters BG, Collis SJ, Chalmers AJ, Joiner MC. 2004. Low-dose hyper-radiosensitivity: a consequence of ineffective cell cycle arrest of radiation-damaged G₂-phase cells. *Radiation Research* 161: 247-255.
- Marples B and Collis SJ. 2008. Low-dose hyper-radiosensitivity: past, present and future. *International Journal of Radiation Oncology Biology Physics* 70: 1310-1318.

Martin F, Caignard A, Jeannin JF, Leclerc A, Martin M. 1983. Selection by trypsin of two sublines of rat colon cancer cells forming progressive or regressive tumours. *International Journal of Cancer* 32: 623-627.

Martin L, Marples B, Coffey M, Lawler, Hollywood D, Marignol L. 2009. Recognition of O6MeG lesions by MGMT and mismatch repair proficiency may be a prerequisite for low-dose radiation hypersensitivity. *Radiation Research* 172: 405-413.

Mothersill C, Harney J, Lyng F, Cotell D, Parsons, Murphy DM, Seymour CB. 1995. Primary explants of human uroepithelium show an usual response to low-dose irradiation with cobalt-60 gamma rays. *Radiation Research* 142, 181-187.

Murphy, MJ, Lin PS, Ozhasoglu C. 2007. Intra-fraction dose delivery timing during stereotactic radiotherapy can influence the radiobiological effect. *Medical Physics* 34: 481-484.

Nuta O, Darroudi F. 2008. The impact of the bystander effect on the low-dose hypersensitivity phenomenon. *Radiation Environment Biophysics* 47: 265-274.

Petrovic I, Ristic-Fira A, Todorovic D, Koricanac L, Valastro L, Cirrone P, Cuttone G. 2010. Response of a radioresistant human melanoma cell line along the proton spread-out Bragg peak. *International Journal of Radiation Biology* 86: 742-751.

Planel H, Soleilhavoud JP, Tixador R, Richoilley G, Conter A, Croute F, Caratero C *et al.* 1987. Influence on cell proliferation of background radiation or exposure to very low, chronic γ radiation. *Health Physics* 52: 571-578.

Rothkamm K, Löbrich M. 2003. Evidence for a lack of DNA double-strand break repair in human cells exposed to very low X-ray doses. *Proceedings of the National Academy of Sciences, USA* 100: 5057-5062.

Slonina D, Biesaga B, Urbanski K, Kojs Z. 2007. Low-dose radiation response of primary keratinocytes and fibroblasts from patients with cervix cancer. *Radiation Research* 167: 251-259.

Short SC, Bourne S, Martindale C, Woodcock M, Jackson SP. 2005. DNA damage responses at low radiation doses. *Radiation Research* 164: 292-302.

Szumiel I. 2012. Radiation hormesis: autophagy and other cellular mechanisms. *International Journal of Radiation Biology* 88: 629-628.

Thariat J, Vignot S, Bensadoun RJ, Mornex F. 2012. Improvements of ablative local treatments modify the management of the oligometastatic disease. *Cancer Radiotherapy* 16: 325-329.

Thomas C, Buronfosse A, Portoukalian J, Fertil B. 1997. The gangliosides as a molecular coupling factor between the proportion of radiosensitive cells *in vitro* and the metastatic potential *in vivo* within a human melanoma cell line. *British Journal of Cancer* 75: 639-649.

Thomas C, Buronfosse A, Courdi A, Fertil B. 2001. Radio-prevention of micrometastasis. *Medical Hypothesis*. 57: 398-404.

Thomas C, Fertil B, Foray N. 2007. Very low-dose hyper-radiosensitivity: impact for radiotherapy of micrometastases. *Cancer Radiotherapy* 11: 260-265.

Thomas C, Charrier J, Massart C, Cherel M, Fertil B, Barbet J, Foray N. 2008. Low-dose hyper-radiosensitivity of progressive and regressive cells isolated from a rat colon tumour: impact of DNA repair. *International Journal of Radiation Biology* 84: 533-548.

Tsoulou E, Baggio L, Cherubini, Kalfas CA. 2001. Low-dose hypersensitivity of V79 cells under exposure to ^4He ions of different energies: survival and chromosome aberrations. *International Journal of Radiation Biology* 77: 1133-1139.

Vaganay-Juery S, Muller C, Marangoni B, Abdulkarim B, Deutsch E, Lambin P, Calsou P, Eschwege F, Salles B, Joiner MC, Bourhis J. 2000. Decreased DNA-PK activity in human cancer cells exhibiting hypersensitivity to low-dose irradiation. *British Journal of Cancer* 83:514-518.

Wéra AC, Borlon C, Nuttens VE, Riquier H, Feron O, Michiels C, Lucas S. 2012. Comparison of the clonogenic survival of A549 non-small cell lung adenocarcinoma cells after irradiation with low-dose-rate beta particles and high-dose-rate X-rays. *International Journal of Radiation Biology* 88: 253-257.

Wykes SM, Piasentin E, Joiner MC, Wilson GD, Marples B. 2006. Low-dose hyper-radiosensitivity is not caused by a failure to recognize DNA double-strand breaks. *Radiation Research* 165: 516-524.

Xue L, Yu D, Furusawa Y, Cao J, Okayasu R, Fan S. 2009. ATP-dependent hyper-radiosensitivity in mammalian cells irradiated by heavy ions. *International Journal of Radiation Oncology Biology Physics* 75: 235-243.

Table I. Major radiobiological studies on HRS/IRR response. Most studies used tumour cell lines. Few studies used transformed cell lines (V79, CHO-K1, MR4, GM0639, EBS7YZ5) or a normal fibroblast cell line (BJ). The doses at which the maximal HRS and IRR response are observed (D_{HRSmax} , D_{IRRmax}) and the time at which the maximal HRS and IRR response are observed (t_{HRSmax} , t_{IRRmax}) were obtained from survival data reported in the quoted references.

Irradiation	Dose rate (mGy.min⁻¹)	D_{HRSmax} (mGy)	t_{HRSmax} (s)	D_{IRRmax} (mGy)	t_{IRRmax} (s)	Cell line	Reference
240 KV X-rays	180	200	67	600	200	Human HT29	Lambin et al. (1993)
240 KV X-rays	118	120	40	500	167	Human Be11	Lambin et al. (1996)
240 KV X-rays	180	250	83	500	167	Human RT112	Lambin et al. (1996)
⁶⁰ Co γ -rays	580	200*	21	600	62	Human variant 1 (T1p26)	Thomas et al. (1997)
⁶⁰ Co γ -rays	580	100*	10	200	21	Human clone 4 (T1C3)	Thomas et al. (1997)
⁶⁰ Co γ -rays	1000	440	26	750	45	Rodent V79	Tsoulou et al. (2001)
9.5Mev α -rays	1000	340	20	500	30	Rodent V79	Tsoulou et al. (2001)
300 KV X-rays	500	110	13	500	60	Rodent subline CHO-K1	Bartkowiak et al. (2001)
⁶⁰ Co γ -rays	2000	100	3	500	15	Human	Chandna et al. (2002)

						BMG1	
⁶⁰ Co γ-rays	2000	200	6	500	15	Human U87	Chandna et al. (2002)
⁶⁰ Co γ-rays	2000	300	9	500	15	Human PECA4451	Chandna et al. (2002)
⁶⁰ Co γ-rays	2000	300	9	1000	30	Human PECA4197	Chandna et al. (2002)
10 MV X-rays	2430	800	20	950	23	Human G5	Beauchesne et al. (2003)
10 MV X-rays	2430	700	17	800	20	Human G111	Beauchesne et al. (2003)
10 MV X-rays	2430	700	17	950	23	Human G142	Beauchesne et al. (2003)
10 MV X-rays	2430	800	20	950	23	Human G152	Beauchesne et al. (2003)
¹³⁷ Cs γ-rays	220	100	27	200	54	Human A549	Enns et al. (2004)
¹³⁷ Cs γ-rays	220	250	68	750	205	Human T98G	Enns et al. (2004)
320 KV X-rays	750	180	14	300	24	Rodent MR4	Wykes et al. (2006)
320 KV X-rays	750	105	8	400	32	Human M059K	Wykes et al. (2006)
320 KV X-rays	750	140	11	400	32	Human EBS7YZ5	Wykes et al. (2006)
⁶⁰ Co γ-rays	660	280	25	1000	91	Human T47D	Edin et al. (2007)
320 KV X-rays	750	310	25	750	60	Human	Krueger et al. (2007a)

						T98G	
⁶⁰ Co γ -rays	1800	100	3.3	300	10	Human BJ	Nuta & Darroudi (2008)
⁶⁰ Co γ -rays	500	190	23	500	60	Rodent PRO	Thomas et al. (2008)
200 KV X-rays	500	100	12	300	36	Human GM0639	Xue et al. (2009)
290 Mev ⁶ C	500	170	20	400	48	Human GM0639	Xue et al. (2009)
62 Mev protons	15000	2000	8	4000	16	Human HTB140	Petrovic et al. (2010)
250 KV X-rays	855	250	18	500	35	Human A549	Wera et al. (2012)

*these numbers correspond to a reanalysis of our raw data for exposure times less than 10 min.

Table II. Dose-rates, exposure times and doses investigated in this study with ^{60}Co γ -rays (data shown in figure 1A-F).

Dose-rate (mGy/min)	Exposure times (s)	Doses (mGy)
230	2.6; 6.5; 13; 26; 65; 78; 130	10; 25; 50; 100; 250; 300; 500
60	5; 10; 25; 50; 100; 200; 300; 500	5; 10; 25; 50; 100; 200; 300; 500
44	7; 14; 27; 70; 140; 270; 341	5; 10; 20; 50; 100; 200; 250
25	6; 12; 24; 60; 120; 180; 240	2.5; 5; 10; 25; 50; 75; 100
0.3	5; 10; 20; 40; 100; 200	0.025; 0.05; 0.1; 0.2; 0.5, 1
0.0025	2.4; 6; 12; 24; 48; 120; 240	0.0001; 0.00025; 0.0005; 0.001; 0.002; 0.005; 0.01

Table III. Values of parameters obtained from the survival data fit to the IR model; α_s represents the initial slope of the curve at very low doses; α_r represents the low-dose slope of the survival curve extrapolated from high-doses; d_c represents the dose that induced the change from HRS to IRR response and β_r represents the distal slope of the survival curve. Numbers in parentheses are the standard errors given by the JMP software; nc = no convergence.

	α_s	α_r	α_s/α_r	d_c (mGy)	β_r
Fig 1A	9.96 (2.1)	0.43 (0.23)	18	42 (8)	0.124 (0.5)
Fig 1B	21.8 (3.5)	0.21 (0.13)	106	21 (2.6)	0.21 (0.31)
Fig 1C (PRO cells)	17.2 (1.2)	0.5 (0.17)	34	23 (1.7)	0.11 (0.74)
Fig 1C (REG cells)	nc	nc	nc	nc	nc
Fig 1D	31.5 (1.6)	1.5 (0.3)	21	11 (0.7)	1.22 (3.45)
Fig 1E	4.05 (0.69)	0.1 (0.03)	41	0.045 (0.006)	-0.024 (0.033)
Fig 1F (PRO cells)	0.59 (0.2)	0.017 (0.016)	35	0.00071 (0.0002)	-0.0006 (0.0018)
Fig 1F (REG cells)	nc	nc	nc	nc	nc
Figure 3A (75 kV X-rays)	55.8 (5.7)	1.36 (1)	41	11 (1.2)	4.9 (10.4)
Figure 3A (^{60}Co γ -rays)	31.5 (1.6)	1.5 (0.3)	21	11 (0.7)	1.22 (3.45)

Table IV. Values of the HRS/IRR response parameters obtained with PRO cells irradiated with ^{60}Co γ -rays. D_{HRSmax} and D_{IRRmax} are the doses at which the maximal HRS and IRR response are observed, respectively; t_{HRSmax} and t_{IRRmax} are the time at which the maximal HRS and IRR response are observed, respectively.

Dose-rate (mGy.min⁻¹)	D_{HRSmax} (mGy)	t_{HRSmax} (s)	D_{IRRmax} (mGy)	t_{IRRmax} (s)
500	$190 \pm 8.1^{\text{a}}$	$23 \pm 1^{\text{a}}$	500^{a}	60^{a}
	250^{b}	30^{b}	500^{b}	60^{b}
230	$42 \pm 8^{\text{a}}$	$11 \pm 2^{\text{a}}$	175^{a}	46^{a}
	$37 \pm 12^{\text{b}}$	$10 \pm 3^{\text{b}}$	$217 \pm 17^{\text{b}}$	$65 \pm 4^{\text{b}}$
60	$21 \pm 2^{\text{a}}$	$21 \pm 2^{\text{a}}$	125^{a}	125^{a}
	$28 \pm 12^{\text{b}}$	$28 \pm 12^{\text{b}}$	$83 \pm 17^{\text{b}}$	$83 \pm 17^{\text{b}}$
44	$23 \pm 2^{\text{a}}$	$31 \pm 3^{\text{a}}$	100^{a}	136^{a}
	27^{b}	37^{b}	55^{b}	75^{b}
25	$11 \pm 1^{\text{a}}$	$26 \pm 2^{\text{b}}$	50^{a}	120^{a}
	17^{b}	41^{b}	38^{b}	91^{b}
0.3	$0.045 \pm 0.006^{\text{a}}$	$9 \pm 1^{\text{a}}$	0.2^{a}	40^{a}
	$0.031 \pm 0.006^{\text{b}}$	$6 \pm 1^{\text{b}}$	$0.19 \pm 0.1^{\text{b}}$	$38 \pm 20^{\text{b}}$
0.0025	$0.00071 \pm 0.0002^{\text{a}}$	$17 \pm 5^{\text{a}}$	0.004^{a}	96^{a}
	$0.0005 \pm 0.00025^{\text{b}}$	$12 \pm 6^{\text{b}}$	$0.002 \pm 0.0009^{\text{b}}$	$48 \pm 22^{\text{b}}$

^a Parameters obtained from survival data fit to the IR model.

^b Experimental parameters obtained from raw survival data shown in Figure 1 except those at 500 mGy.min⁻¹ (taken from Thomas et al. 2008)

Legend to figures

Figure 1. Impact of dose-rate on the HRS/IRR response. Survival curves of PRO cells (A-F) and REG cells (C and F) irradiated with cobalt 60 γ -rays at low-doses. Experiments were performed with cells cultured for no more than five passages ($p < 5$). Each data represents the mean \pm SEM of three (A), three (B), two (PRO cells) and two (REG cells) (C), two (D), four (E) and three (F) experiments for cells irradiated 24h after plating. Six data points per dose are included in each experiment. Figures were fitted to a smooth function. * $p < 0.05$ for comparison between irradiated cells and unirradiated cells, using the t-test.

Figure 2. Relationships between the HRS/IRR response experimental parameters (shown in Table IV) and the dose-rates in PRO cells. (A) Significant linear correlation between D_{HRSmax} and dose-rate was found ($y = 0.4428.x$, $R^2 = 0.89$, $p < 0.05$). (B) t_{HRSmax} was not significantly correlated to dose-rate. (C) Significant linear correlation between D_{IRRmax} and dose-rate was found ($y = 0.997.x$, $R^2 = 0.99$, $p < 0.05$). (D) t_{IRRmax} was not significantly correlated to dose-rate. Error bars indicate the SEM for $n = 2-4$ independent experiments taken from figures 1A-F (■) and for 25 independent experiments obtained with low-LET radiation taken from table I (□).

Figure 3. HRS/IRR response of PRO cells irradiated with 75 kV X-rays. (A) Comparison between ^{60}Co γ -rays survival data (dashed line) and 75 kV X-rays survival data (continuous line). Experiments were performed with cells cultured for no more than 5 passages. Each data represents the mean \pm SEM of two independent experiments for cells irradiated 24h after plating. Six data points per dose are included in each experiment. * $p < 0.05$ for comparison between unirradiated cells and irradiated cells using the t-test. (B) Kinetic of DSB repair at 10 mGy (HRS response) or 100 mGy (IRR response). Each data represent the mean \pm SEM of 3-5 independent experiments for cells irradiated 24 h after plating. All data in figure 3 were fitted to a smooth function.

Figure 4. Model for the HRS/IRR response. From 0 to D_{HRSmax} , radiations induce physical DSB that are not all recognized biologically and therefore unrepaired. Consequently, cell survival decreases. From D_{HRSmax} to D_{IRRmax} , DSB are all recognized biologically and progressively repaired and cell survival increases. For doses higher than D_{IRRmax} , DSB are all recognized but their amount is so large that some DSB are not repaired and cell survival decreases.

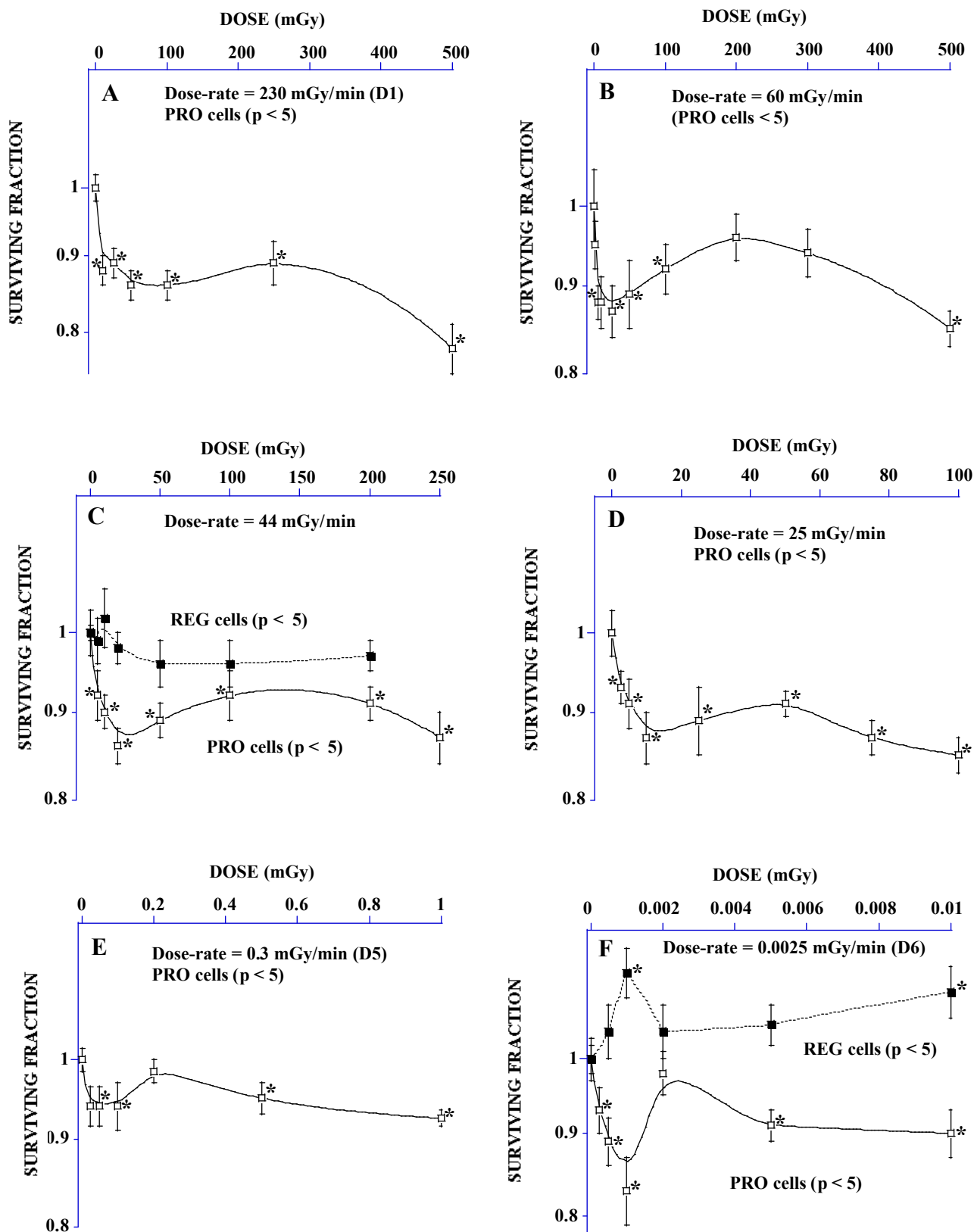


Figure 1

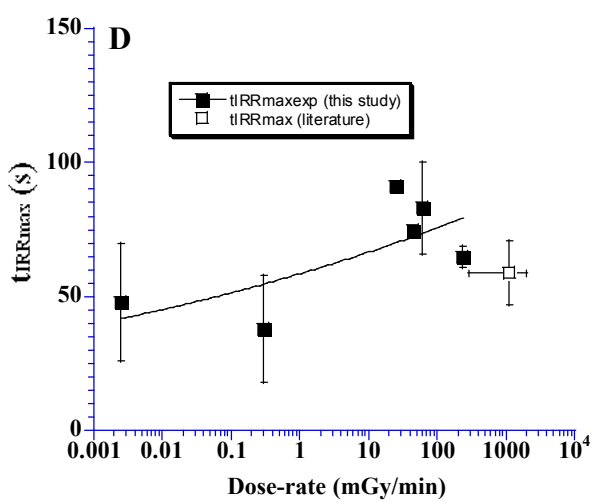
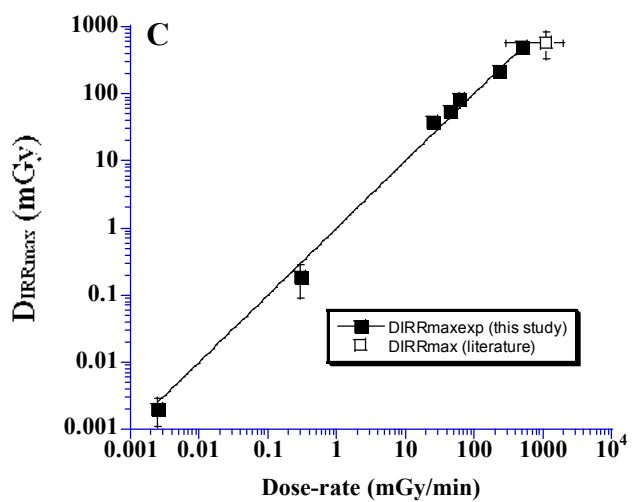
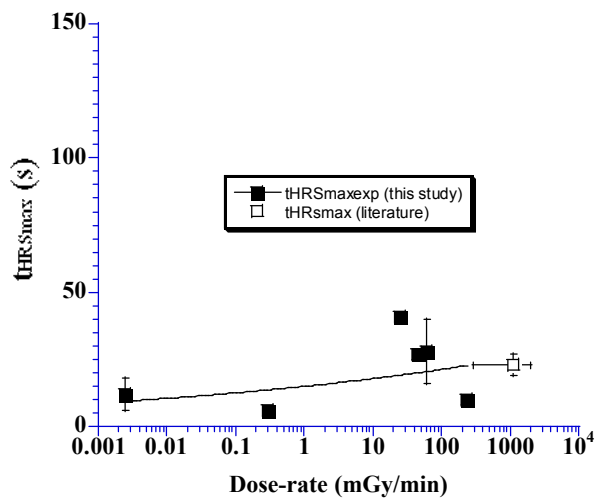
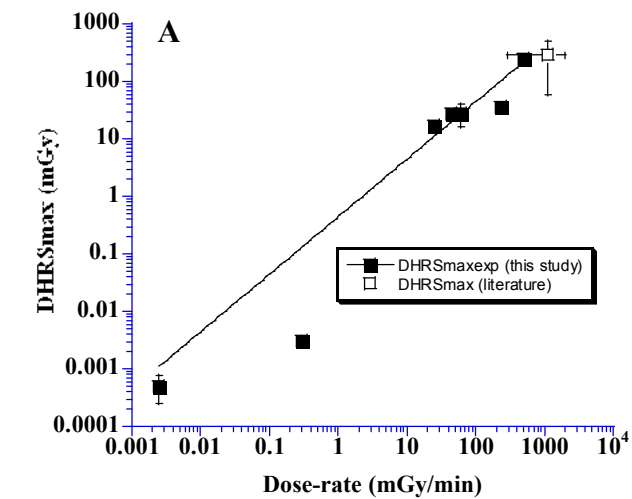


Figure 2

Figure 3

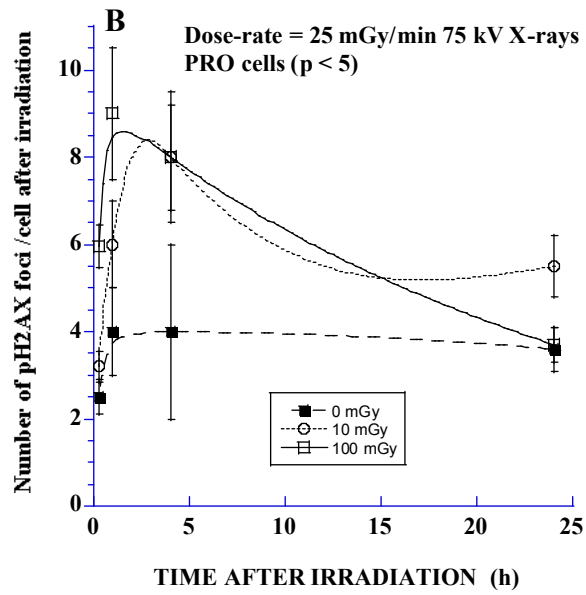
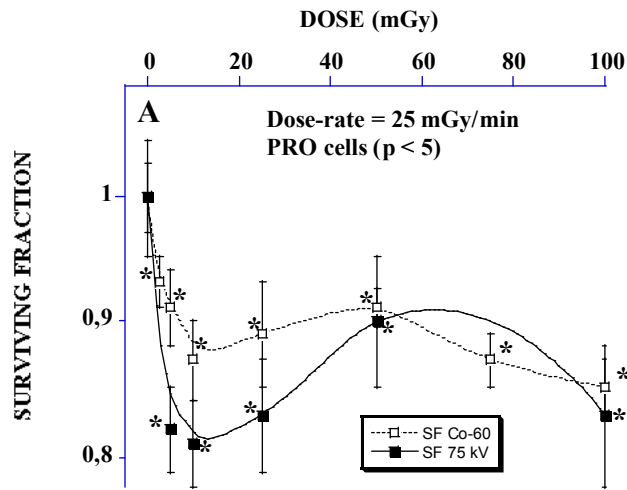


Figure 4

